Analytic Model of Reactive Flow

P. Clark Souers, Peter Vitello

November 18, 2004

Propellants, Explosives, Pyrotechnics

Disclaimer

Analytic Model of Reactive Flow

P. Clark Souers and Peter Vitello

Energetic Materials Center, Lawrence Livermore National Laboratory, Livermore, CA USA 94550

Abstract

A simple analytic model allows prediction of rate constants and size effect behavior before a hydrocode run if size effect data exists. At infinite radius, it defines not only detonation velocity but also average detonation rate, pressure and energy. This allows the derivation of a generalized radius, which becomes larger as the explosive becomes more non-ideal. The model is applied to near-ideal PBX 9404, in-between ANFO and most non-ideal AN. The power of the pressure declines from 2.3, 1.5 to 0.8 across this set. The power of the burn fraction, F, is 0.8, 0 and 0, so that an F-term is important only for the ideal explosives. The size effect shapes change from concave-down to nearly straight to concave-up. Failure is associated with ideal explosives when the calculated detonation velocity turns in a double-valued way. The effect of the power of the pressure may be simulated by including a pressure cutoff in the detonation rate. The models allows comparison of a wide spectrum of explosives providing that a single detonation rate is feasible.

Keywords: model, reactive flow, detonation rate, size effect, diameter effect

1 Introduction

Reactive Flow is the class of explosive models where the chemistry of detonation is simulated by an overall reaction rate and where the rate constant is assumed to be truly constant. Although these models have been in use for thirty years, their workings often seem mysterious. Moreover, once calibrated for one explosive, it is not obvious how to change the parameters for another. The simple analytic model given here works for many explosives providing that a single detonation rate can be used.

The test of this model is to calculate the size (diameter) effect, which is a plot of detonation velocity versus inverse radius of a cylindrical explosive part. The spectrum of explosives may be indicated by considering three general classes, all very different.   1) Ideal PBX 9404 and Comp B have a shape that is strongly concave-down in inverse radius space. The explosives fail at 0.6–2 mm with a dimensionless detonation velocity U_s/D ratio of 0.83-0.85.[1,2]   2) Non-ideal ammonium nitrate emulsion k1a and ANFO prill have an almost straight size effect line, and they fail at a radius of 6-10 mm with U_s/D of about 0.6.[3-5]   3) Extremely non-ideal ammonium nitrate at 1.0 g/cm^3 and Australian heavy ammonium nitrate emulsion, HANFO, are concave-up in shape, fail at 25-70 mm with U_s/D of 0.25-0.31.[6,7] Thus, the radii get larger and failure occurs at lower fractional detonation velocities. In the simple reactive flow code JWL++, these three, calculated separately, have usually had detonation rates with powers of the pressure, b, of 2-3, 1 and 1, respectively.[8]

To model size effect behavior, Leiper, Kirby and Cooper suggested a Gaussian function that modulates the energy delivery over the range of the burn fraction, F. [9-11] In their one-dimensional, three-rate model, they reproduced the concave-up size effect shape of AN slurry and nitrogylcerine powder using a Gaussian function peaked at the early burn fraction of 0.15. They also reproduced the concave-down shape of Comp B with a late energy delivery peak at a burn fraction of 0.7. Their Gaussian functions did not run continuously from $0 < F < 1$ but turned on at some initial value of F. The rate was proportional to pressure to the first power. This approach showed that energy delivery early or late in the reaction zone can set the shape of the size effect curve.

2 Necessary Input Relations

The model assumes that a burn fraction, F, of 1 occurs only for detonation of a ratesticks of infinite radius, where the detonation velocity is D. All real ratesticks of radius R_o have a smaller detonation velocity U_S. The sonic surface at the back of the reaction zone, then, is never at $F = 1$, although the explosive may burn the rest of the way behind the reaction zone, where it goes not affect the detonation front. The burn fraction at the back of the reaction zone, F_e, is related to the other variables by this useful equation, which is more fully discussed in the Appendix:

$$F_e \approx \frac{E_o}{E_D} \approx \frac{P_m}{P_D} \approx \left(\frac{U_S}{D}\right)^2 \tag{1}$$

where the numerators are all at the radius R_o and the denominators are all at infinite radius. In a reactive flow code, F is defined in terms of the fraction of the detonation energy, E_o. P_m is a mean pressure somewhere between the spike and the C-J point.

Ratestick detonation velocities are described by this equation from Eyring, et. al.[12]

$$U_S = D\left(1 - \frac{<x_e>}{\sigma R_o}\right) \tag{2}$$

where $<x_e>$ is the average reaction zone length. The extrapolation of this inverse radius plot back to zero is what defines D.   The reaction zone length is equated with measured edge lags of the detonation front, and the parameter σ is empirically described by[13]

$$\sigma = \frac{0.4}{\left(1-(U_S/D)^2\right)^{0.8}}.$$

(3)

Also, the time to cross the reaction zone, t_e, is given by

$$t_e = \frac{<x_e>}{U_S}.$$

(4)

3 The Simple Model

The rate equation for a one-rate model is

$$\frac{dF}{dt} = GP^b F^a (1-F)^c$$

(5)

where G is the rate constant, which can be a function of the radius and, therefore, not really a constant. We collect F on the left and integrate numerically to F_e to get the result

$$I = \int_0^{F_e} \frac{dF}{F^a(1-F)^c} \approx G\left(P_D F_e\right)^b t_e.$$

(6)

In the reaction zone, the pressure declines from the spike to the C-J point, but we shall use a mean pressure for simplicity. We substitute Eqs. (1), (2) and (4) to get

$$I = R_o\left(\frac{G}{D}\left(P_D\right)^b\right)\sigma\left(F_e^{b-1/2}(1-F_e^{1/2})\right).$$

(7)

We define a dimensionless radius

$$R_D = \frac{D}{G_D(P_D)^b}.$$

(8)

We now replace G with G_D, which will be held constant for all radii. G_D is obtained by extrapolating G back to zero inverse radius. We rearrange Eq. (7) to get

$$\frac{R_D}{R_O} = \frac{\sigma}{I} F_e^{(b-1/2)} (1 - F_e^{1/2}) \; .$$ (9)

Eq. (9) now becomes a generalized version of the Eyring equation. We will solve it for R_D/R_o against which we will plot versus the dimensionless detonation velocity U_s/D.

4 Estimating G_D

How do we estimate the constant G_D from real data? The average detonation rate is inversely proportional to the slope of the size effect curve.[8] This effect is easily seen in the codes by changing rates and watching the curves rotate about the infinite-radius detonation velocity, D. We take Eq. (5) and convert it to the average detonation rate for a radius R_o

$$\left\langle \frac{dF}{dt} \right\rangle \approx \frac{-DU_S}{\partial U_S / \partial(1/R_O)} \approx G\left(P_D <F_e> \right)^b <F>^a <1-F>^c \; .$$ (10)

where $<dF/dt>$ in μs^{-1} is independent of models. The average value $<F>$ is set to be 1/2. We next move to infinite radius, where $F_e = 1$, so that term disappears. The middle term takes size effect data and converts it into an average rate, which we then extrapolate back to zero inverse radius to get the average rate at infinite radius $<dF/dt>_D$. Also, G turns into G_D, now a true constant. We have a problem with the averages of the terms containing F. First, we are not sure what value to use if evaluated at infinite radius. Second, the terms are function of a and c, which is extremely inconvenient in repetitive calculating and plotting. We shall try an intermediate position, where we use the a = 0, c = 1 value of 1/2 everywhere. We then get at infinite radius

$$G_D \approx \frac{2}{\left(P_D \right)^b} \left\langle \frac{dF}{dt} \right\rangle_D = cons\tan t \; .$$ (11)

We see that $G_D(P_D)^b$ and R_D are indeed constant with respect to b, which is an important relation. This produces the effect where if b increases, so does G_D. It is well-known in a reactive flow code that increasing the power of the pressure causes the rate constant to also increase exponentially. We get the generalized radius

$$R_D \approx \frac{D}{2 < dF/dt >_D} \tag{12}$$

in terms of the size effect data as discussed after Eq. 10.

5 Results

The near-ideal, concave-down explosive PBX 9404 is shown in Figure 1. The bend is so great that the entire curve lies in a small R_D/R_o range. To get this effect, we need a large value of a = 0.67 and of b = 2.3, and this is shown by the heavy line.

The less ideal explosives have a nearly straight line as shown in Figure 2: AN emulsion k1a and ANFO prill. These are easily fit with a = 0, c = 1 and b = 1.5.

Figure 3 goes to other extreme at large R_D/R_o values with the ultra-slow, super non-ideal explosives 1.0 g/cc AN, potassium chlorate 80/sugar [14] and HANFO (Australian heavy AN emulsion). We use a = 0, c = 1, b = 0.8 to get a concave-up shape.

We have fit all three kinds of explosives by increasing b going from non-ideal to ideal explosives. It is interesting to note that $F^{0.67}$ was derived as a description of energy spherically moving outward from hot spots,[12] yet it appears here only for the most ideal case. Increasing a or b causes the curve to become more concave-down in slightly different ways. PBX 9404 is so concave-down that both terms have been made large.

6. Pressure Cutoff

Leiper, et. al. made an analytical model that used b = 1 with a pressure cutoff P_o to create the concave-down shape as well as failure. [9-11]   For P < P_o, G_D = 0. This can be added to give

$$R_D = \frac{D}{G_D(P_D - P_o)^b}. \tag{13}$$

The result is shown by the fine line in Figure 1, where the concave-down shape is given with b = 1 with $P_o = 0.3P_D$. A large value of a is still needed. The pressure cutoff is yet another way to create concave-down behavior. This applies only in the region of small R_D/R_o, a double-valued curve appears, of which the cusp is often taken as indicating failure.

7. Summary

We have constructed a simple model for detonation in the Reactive Flow manner, and we have used this model to calculate size effect curves. The model assumes that energy is proportional to pressure which is proportional to detonation velocity-squared. It also assumes total reaction only at infinite radius and expects ever smaller burn fractions as the radius decreases. The shape of the size effect curve is set by the powers of the pressure, the burn fraction and one minus the burn fraction- all of which describe the energy delivery inside the reaction zone. Ideal explosives show concave-down size effect curves and extremely non-ideal explosives show concave-up curves. In going from ideal to non-ideal, the power of the pressure (b) continually declines. The power of the burn fraction (a) can be large only for ideal explosives. In summary, the model shows that this simple method can be used across the spectrum of explosives.

Appendix
A1 Deriving the Energy-Pressure-Detonation Velocity Relation

Eq. (1), which is essential for this model, is an approximate but useful equation for scaling of equations-of-state. The relation

$$F \approx \frac{E_o}{E_D} \tag{A-1}$$

is true by definition. If we consider with the mass-momentum conservation equation

$$(1 - v_{cj}) = \frac{u_p}{U_s}, \tag{A-2}$$

we find from the thermochemical code CHEETAH that the C-J relative volume for most dense explosives is 0.76-0.78 and for half-dense 0.72-0.73. If we take a _ compression as the average, we have

$$u_p \approx U_S . \tag{A-3}$$

We next use the density-momentum conservation equation

$$P = \rho_o U_S^2 (1 - v) \tag{A-4}$$

and compare results at radius R_o with infinite radius to get

$$\frac{P_m}{P_D} \approx \left(\frac{U_S}{D}\right)^2 . \tag{A-5}$$

Next, we consider that E_o, before it comes out of the explosive to do work, must be used to compress and accelerate the mass of the unreacted explosive next to it. We set

$$E_O \approx P(1 - v) . \tag{A-6}$$

We next substitute Eqs. (A-3) and (A-4) and add infinite radius to get

$$\frac{E_O}{E_D} \approx \left(\frac{U_S}{D}\right)^2 . \tag{A-7}$$

A2   Relations in the Model

Because we have no real data to test the above relations, we turn to the reactive flow model JWL++ running in a two-dimensional arbitrary Lagrangian-Eulerian (ALE) hydrocode with CALE-like properties. We shall run different radii of the same material. The sonic plane is found using the function

$$(u_{px}^2 + u_{py}^2)_i^{1/2} + C_i - U_S = 0 . \tag{A-8}$$

where U_s is the detonation velocity in the ratestick found in the first code run and C_i is the speed of sound as determined by the equation-of-state. The particle velocities and sound speeds are in the ith zone on every cycle, so that their sum forms an instantaneous detonation velocity. When Eq. (A-9) equals zero, we are on the sonic plane, where no energy can move forward to the front. In a given zone, we plot the burn

fraction versus the sonic function to get the burn fraction on the sonic plane. The maximum pressures are also obtained wherever they appear inside the reaction zone. The averages for the overall burn fraction and maximum pressure are given by

$$\langle F_e \rangle = \sum_i \lambda_i F_{ei}$$
$$\langle P_m \rangle = \sum_i \lambda_i P_{mi}$$

(A-9)

.

where λ_i is the fraction of radial area. We need to use explosives that have large reaction zones and react at small burn fractions in order to get the resolution possible in mapping code output. The zoning is set so that we have a 35-50 zones radially and that the reaction zone contains 8 –12 zones. At least 12 slices and sometimes over 20 slices radially are taken in the analysis. For ratesticks 10 times longer than the radius, the results are constant at each radius and represent steady state conditions. The values of D and P_D come from extrapolation of the code results with the running of a large radius sample being essential to obtaining a good value.

The results are plotted in Figure 4. The linear relations agree with the derivations we carried out.

References

[1]   *LASL Explosive Property Data*, T. R. Gibbs and A. Popolato, ed., University of California Press, Berkeley, **1980**.

[2]   M. E. Malin, A. W. Campbell and G. W. Mautz, Particle Size Effects in One- and Two-Component Explosives, *Second ONR Symposium on Detonation,* White Oak, MD, February 11, **1955**, pp. 478-493.

[3]   U. Nyberg, J. Deng and L. Chen, *Matning av Detonationshastighet och Krokningsfront i Samband med Brinnmodellutveckling for Emulsionssprangamne K1*, Swedish Rock Engineering Research, Stockholm, SveBeFo Report 6, **1995**.

[4]   J. Deng, S. Nie and L. Chen, *Determination of Burning Rate Parameters for an Emulsion Explosive*, Swedish Rock Engineering Research, Stockholm, SveBeFo Report 17, **1995**. Finn Ouchterlony kindly sent the Swedish Rock reports.

[5]   Richard Catanach, Los Alamos National Laboratory, Los Alamos, NM, private communications, **2002-2003**.

[6]   M. A. Cook, E. B. Mayfield and W. S. Partridge, Reaction Rates of Ammonium Nitrate in Detonation, *J. Phys. Chem.* **1955** *59*, 675-680.

[7]   David Kennedy, ICI Australia Operations, Kurri Kurri, New South Wales, Australia, private communications, **1995, 1997**.

[8]   P. Clark Souers, Steve Anderson, Estella McGuire, Michael J. Murphy, and Peter Vitello, Reactive Flow and the Size Effect, *Propellants, Explosives, Pyrotechnics* **2001***, 26*, 26-32.

[9]   I. J. Kirby and G. A. Leiper, A Small Divergent Detonation Theory for Intermolecular Explosives, *Proceedings Eighth Symposium (International) on Detonation*, Albuquerque, NM, July 15-19, **1985**, pp. 176-186.

[10] G. A. Leiper and J. Cooper, Reaction Rates and the Charge Diameter Effect in Heterogeneous Explosives, *Proceedings Ninth Symp[osium (International) on Detonation*, Portland, OR, August 28- September 1, **1989**, pp. 197-207.

[11] G. A. Leiper, Aberdeen, U. K., private communications, **2002-2003**.

[12]   H. Eyring, R. M. Powell, G. E. Duffey and R. B. Parlin, The Stability of Detonation, *Chem Rev* **1949***, 45*, 144-146.

[13] P. Clark Souers and Raul Garza, Kinetic Information from Detonation Front Curvature, *Proceedings Eleventh International Detonation Symposium*, Snowmass Village , CO, August 30-September 4, **1998**, pp. 459-465.

[14] Raul Garza and P. Clark Souers, Lawrence Livermore National Laboratory, private communication, **2003**.

Symbols and Abbreviations

a	Pressure exponent for F (dimensionless)
b	Pressure exponent for pressure (dimensionless)
C	Speed of sound (mm/μs)
c	Pressure exponent for (1- F) (dimensionless)
D	Detonation velocity at infinite radius (mm/μs)
E_o	Detonation energy at radius R_o (kJ/cm^3)
E_D	Detonation energy at infinite radius (kJ/cm^3)
F	Burn fraction (dimensionless)
$<F>$	Average burn fraction (dimensionless)
$<dF/dt>$	Average detonation rate (μs^{-1})
$<dF/dt>_D$	Average detonation rate at infinite radius (μs^{-1})
F_e	Burn fraction at the back of the reaction zone (dimensionless)
G	Rate constant at radius R_o (μs$\cdot$GPa^{b1})$^{-1}$
G_D	Rate constant at infinite radius (μs$\cdot$GPa^{b1})$^{-1}$
I	Integral of all F-terms (dimensionless)
i	Sub indicating ith zone (dimensionless)
P	Pressure (GPa)

P_D	Maximum pressure at infinite radius (GPa)
P_m	Maximum pressure at radius R_o (GPa)
$<P_m>$	Average maximum pressure at radius R_o (GPa)
R_D	Generalized radius (dimensionless)
R_o	Initial explosive radius (mm)
t	Time (μs)
t_e	Time at end of reaction zone (μs)
u_p	Particle velocity (mm/μs)
u_{px}	X-direction particle velocity (mm/μs)
u_{py}	Y-direction particle velocity (mm/μs)
U_s	Detonation velocity at radius R_o (mm/μs)
V	Relative volume (dimensionless)
v_{cj}	Relative volume at the C-J point (dimensionless)
$<x_e>$	Average reaction zone length (mm)
λ	Fraction of radial area (dimensionless)
ρ_o	Initial explosive density (g/cm^3)
σ	Variable that links radius and reaction zone length

Figure captions

Figure 1. Extreme concave-down curve for near-ideal PBX 9404. This takes a large a = 0.67 and b = 2.3, (thick line) or b may be reduced by using a pressure cutoff (thin line).

Figure 2. Somewhat non-ideal AN emulsion k1a (squares) and ANFO prill (circles) with b = 1.5 and a = 0, c = 1. The shape is close to being a straight line.

Figure 3. Concave-up shapes for extremely non-ideal AN (squares), potassium chlorate/sugar (diamonds) and HANFO (circles) with a = 0, c = 1 and b = 0.8.

Figure 4. Code plot of dimensionless detonation velocity-squared and pressure as a function of the burn fraction. The results are close to linear for both functions. The symbols indicate dimensionless detonation velocity (circles) and dimensionless pressure (squares).
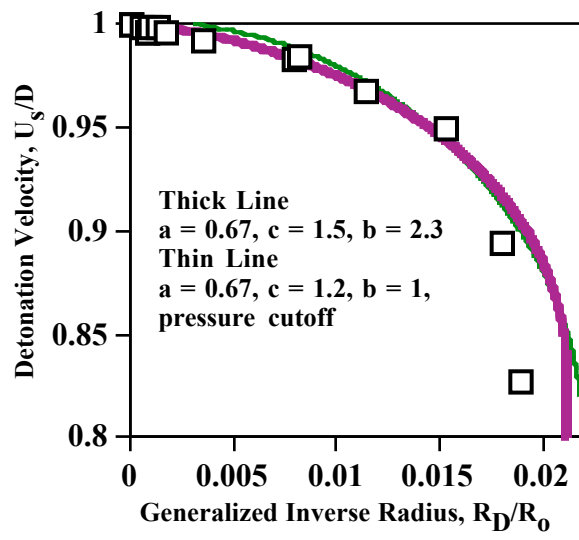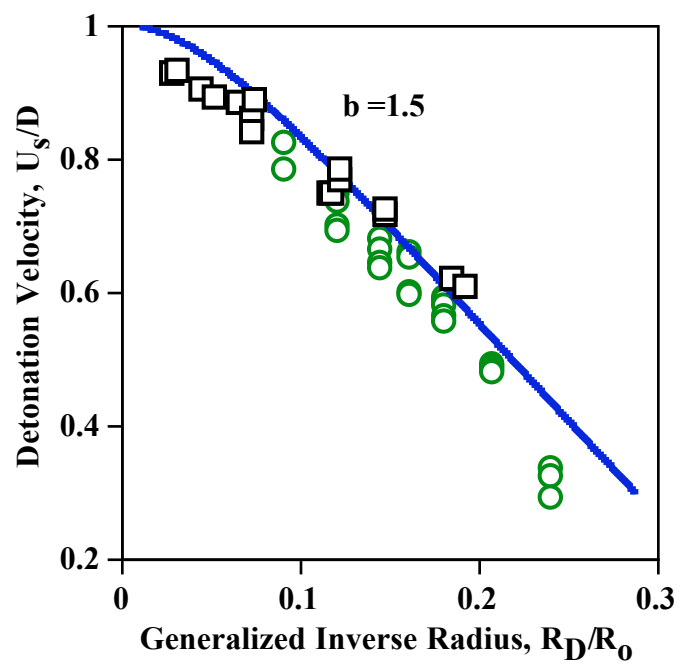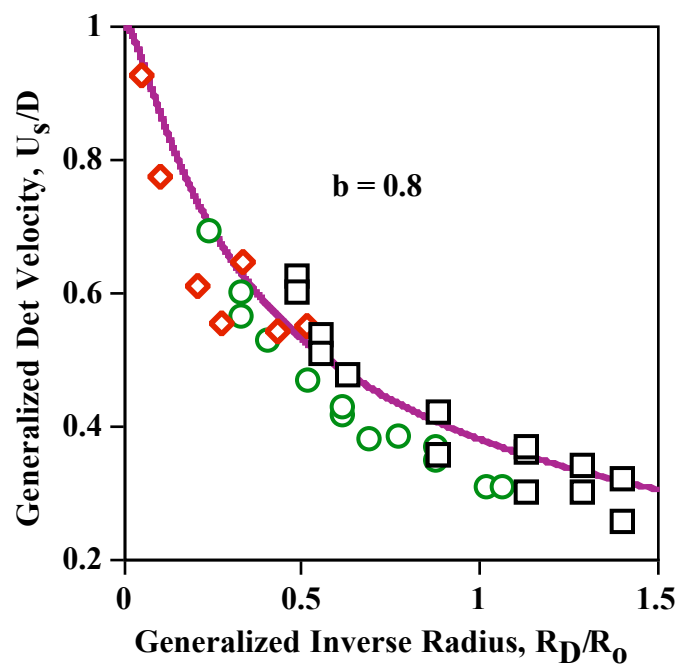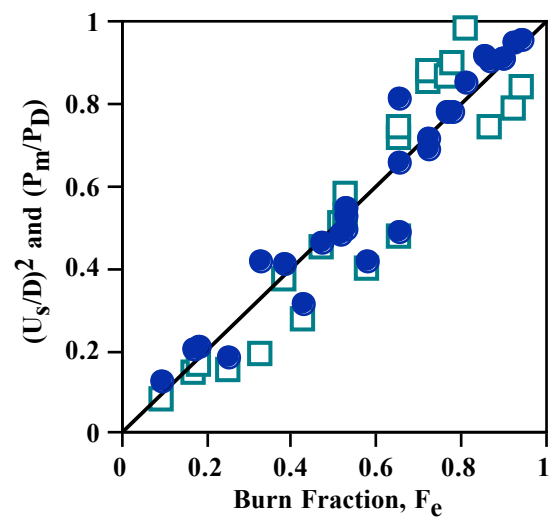
Figure 1

Figure 2.

Figure 3.

Figure 4.